tions. When grown at 8°C the sample droplets are equilibrated against a reservoir of 50 percent saturated ammonium sulfate, while those grown at room temperature are equilibrated against 65 percent saturated ammonium sulfate.

The yeast $tRNA^{fMet}$ crystals grow in three main forms: flat diamond-shaped sheets, tetragonal bipyramids, and hexagonal prisms. Only this last form (Fig. 2) has given useful x-ray diffraction patterns. These crystals form within 1 to 2 weeks with no prior formation of a precipitate as in the case of *E. coli* $tRNA^{Leu}$. Since only the hexagonal-prism form has been useful for x-ray diffraction work, conditions were sought to grow this form preferentially. This form can be grown almost to the complete exclusion of the others by slowly (over a 4- to 5-day period) approaching the final concentration of ammonium sulfate in the solvent reservoir with spermine or spermidine as the polyvalent cation in the sample droplet. With the density gradient technique, the density of the hexagonal-prism form of these crystals was 1.29 ± 0.02 g/cm^3. The x-ray data indicate that the unit cell is hexagonal with dimensions 115 by 115 by 137 Å (*2*). Therefore the crystals are about 15 percent tRNA by volume and contain 12 molecules per unit cell. These crystals show the same birefringence as that described for the *E. coli* $tRNA^{Leu}$ crystals.

Crystals were mounted for x-ray diffraction studies by drawing the crystal along with some of the mother liquor into a 0.7-mm quartz capillary. The mother liquor was removed, and the crystal was blotted dry with a filter paper strip. A small volume of solution, identical in composition to the mother liquor but with no tRNA, was added to the end of the capillary which is then sealed with vacuum grease. Crystals of both tRNA's mounted this way have lasted over 100 hours in the x-ray beam with no significant decrease in resolution.

Since this technique consumes only about 0.1 mg of tRNA per experiment, it is possible to survey a large number of crystal growth conditions with a minimum consumption of material. By a survey of the variables described here it has already been possible to significantly improve the thermal and mechanical stability as well as the crystalline order of the tRNA crystals. Efforts are now under way to further improve these crystal characteristics, and when the x-ray data warrant it, this same technique can be used to survey for satisfactory isomorphous replacements.

JAMES D. YOUNG, ROBERT M. BOCK
Department of Biochemistry and
Laboratory of Molecular Biology,
University of Wisconsin, Madison
SUSUMU NISHIMURA
National Cancer Research Institute,
Tokyo, Japan
H. ISHIKURA, Y. YAMADA
Tokyo Medical and Dental University
U. L. RAJBHANDARY
Department of Biology, Massachusetts
Institute of Technology, Cambridge
MINDAUGAS LABANAUSKAS
PETER G. CONNORS
Laboratory of Biophysics,
University of Wisconsin

References and Notes

1. A. Hampel, M. Labanauskas, P. G. Connors, L. Kirkegaard, U. L. RajBhandary, P. B. Sigler, R. M. Bock, *Science* **162**, 1384 (1968).
2. M. Labanauskas, P. G. Connors, J. D. Young, R. M. Bock, J. W. Anderegg, W. W. Beeman, *ibid.*, this issue.
3. This species is the last leucine acceptor eluted from DEAE Sephadex A-50 columns by NaCl gradients. In the NaCl gradient elution of tRNA from BD-cellulose it emerges late but before the fractions requiring elution with 10 percent ethanol. This sample was pure by the criterion of yielding unique oligonucleotides in molar ratios when digested with ribonuclease T-1 but accepted less than the amount of amino acid predicted for a pure species (H. Ishikura, Y. Yamada, S. Nishimura, unpublished observations).
4. T. Lindahl, D. D. Hensley, J. R. Fresco, *J. Amer. Chem. Soc.* **87**, 4961 (1965).
5. U. L. RajBhandary and H. P. Ghosh, *J. Biol. Chem.* **244**, 1104 (1969).
6. Supported by National Institutes of Health grant GM-12395 and National Science Foundation grant GB-6993.

2 September 1969

Structural Studies on Transfer RNA: The Molecular Conformation in Solution

Abstract. *Small-angle x-ray scattering curves from four different species of transfer RNA in solution indicate that the molecules are of very similar size and shape. A model which has regions of the molecule folded tightly around a long helical core gives good agreement with the observed scattering curves.*

We performed small-angle x-ray scattering studies on dilute solutions of three purified species of tRNA (*1*): $tRNA^{fMet}$ (yeast), $tRNA^{Tyr}$ (yeast), and $tRNA^{Phe}$ (*Escherichia coli*). All samples were studied in 0.1*M* KCl, 0.005*M* $MgCl_2$, and 0.02*M* tris-HCl buffer (*p*H 7.2) at 20° to 25°C. Data were taken on a symmetrical four-slit diffractometer (*2*) with slit separations of 50 cm. Scattered intensities were measured for angles between 5.5 and 180 milliradians (mr), corresponding to Bragg spacings between 280 and 8.6 Å. The experimental curves after correction for slit height smearing effects are shown in Fig. 1a, together with the curve obtained under similar conditions from a fraction of yeast tRNA's rich in $tRNA^{Ala}$ (*3*). The $tRNA^{Ala}$ was dissolved in a buffer containing no $MgCl_2$, but without dialysis. It is probable that Mg^{2+} was present on the tRNA. All four species show very similar scattering curves, supporting the idea that most tRNA's have a similar three-dimensional conformation. We find radii of gyration between 23.5 and 25 Å, in agreement with other values (*3, 4*).

Assuming the general validity of the cloverleaf configuration for tRNA, we constructed Corey-Pauling-Koltun space-filling models; coordinates were assigned, and the theoretical, spherically averaged x-ray scattering curves were calculated and compared with the experimental curves. Coordinates used for the helical regions were those for the 11-fold helix model of reovirus double-stranded RNA (*5*). To reduce the computing time, coordinates were assigned only to the scattering centers of base, sugar, and phosphate groups; scattering factors for the groups were determined by summation of the atomic scattering factors for atoms in water (*6*). We have compared scattering curves calculated for segments of double-helical RNA using atomic coordinates with curves calculated from the group approximation, and we found that the group approximation gives curves which are qualitatively correct out to 160 mr. Bound K^+ ions were assigned to phosphate groups, but scattering due to a water and ion cloud shell was ignored. Since the sequence of nucleotides in the tRNA is unimportant for calculating the small-angle scattering curve, models were built to the form of an average tRNA of 78 nucleotides. Helical regions were poly G·poly C, and unpaired bases were about half purines and half pyrimidines.

In a similar model-building study, Lake and Beeman (*3*) had found that the inner region of the scattering curve, to 50 mr, corresponding to radius of

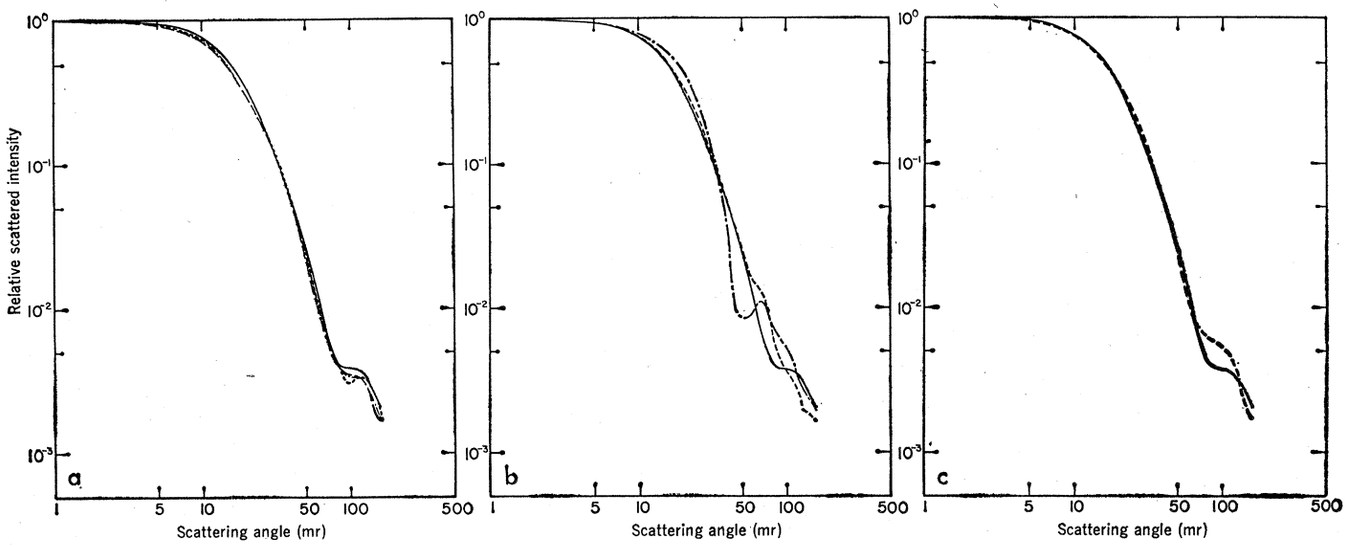

Fig. 1. X-ray scattering curves for tRNA in solution. (a) Experimental scattering from four species of tRNA: yeast $tRNA^{fMet}$ (solid line), yeast $tRNA^{Ala}$ (short-dash line), *E. coli* $tRNA^{Phe}$ (dot-dash line), yeast $tRNA^{Tyr}$ (long-dash line). (b) Experimental scattering from yeast $tRNA^{fMet}$ (solid line) compared to theoretical scattering from H model of Lake and Beeman (*3*) (short-dash line) and theoretical scattering from model of Cramer *et al.* (*7*) (dot-dash line). (c) Experimental scattering from yeast $tRNA^{fMet}$ (solid line) compared to theoretical scattering from model described in text (dash line).

gyration and approximate shape information, could be matched with a model having parallel helical regions with two up, two down (H model); or with three up, one down. Their best fit with an H model is shown in Fig. 1b. A model constructed according to the form given for yeast $tRNA^{Phe}$ by Cramer *et al.* (*7*) gave a theoretical scattering curve which is also shown in Fig. 1b. We describe here a model which gives the theoretical curve shown in Fig. 1c. The agreement with experiment is much improved. The theoretical and experimental curves agree to larger angles and lower intensities than with the Lake and Beeman model, and the shape of the shoulder in the theoretical curve is quite similar to that observed.

In all four experimental curves, the pronounced shoulder at 100 to 130 mr and the absence of any shoulder at smaller angles are characteristic. In seeking a model that would give good agreement with these important characteristics, we discovered that the axial separation of parallel helical segments must be reduced from approximately 20 Å in the H model to about 5 Å. This can be achieved with RNA double helices because the base pairs are offset from the helix axis and because the major groove is much deeper than in the DNA "B" form. Short helical segments of three or four base pairs, if rotated 180° from the neighboring helix, can be inserted without serious distortion in the major groove of a long helix with the two axes separated by as little as 4 Å. All models which we have constructed with large axial separations fail to match these two characteristics (Fig. 1b). Based on these studies, we propose the following model for tRNA.

Starting with the cloverleaf configuration (Fig. 2A), we have made one

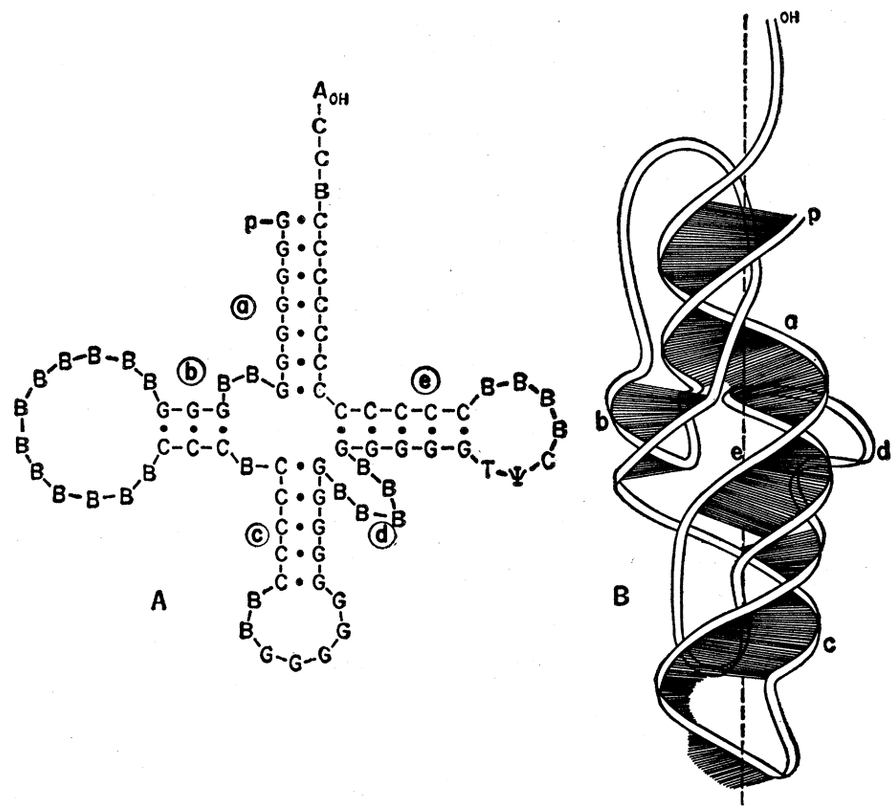

Fig. 2. (A) Cloverleaf configuration of average tRNA used in model calculations. The B is an average unpaired base. The CCA terminus and TψC loop are identified. The bottom loop contains the anticodon. The five unpaired but helically stacked bases in this loop were treated as guanine. The large dihydrouridine loop is on the left. (B) Schematic drawing of proposed model labeled as in Fig. 2A. The dashed line is the long helix axis.

continuous double helix of 12 base pairs out of helix *a* and helix *e* (Fig. 2B). This can be done in all sequenced tRNA's, leaving a break in only one chain of the double helix where the chains turn out to go to helix *b* and the variable arm *d*. This break is easily constructed through rotation about sugar to phosphate bonds without distortion of the main helix. Helical segments *b* and *c* are then placed parallel to the main helix fitting into the large groove of the main helix, with a rotation of 180° between parallel helices. The anticodon arm (helix *c*) is placed at the helix *e* end with the anticodon in the Fuller-Hodgson conformation (*8*) at the extremity of the molecule. This helix can be made coaxial with the main helix by keeping the region of overlap to one base pair or less. When this is done, helix *b* can be moved as far out as 10 Å from the main helix without seriously altering the shoulder region of the scattering curve, but the agreement between the observed and calculated scattering curves is best when helix *b* is placed at an axial separation of about 4.5 Å. This helix is placed in the groove of the helix *e* section of the main helix, situated near the break in the main helix, with the dihydrouridine loop of helix *b* extending in the direction of the CCA hydroxyl end. The shortest distance between phosphates of neighboring helical segments is about 5.5 Å, which might require a divalent cation for stability. This would agree with the findings of Lindahl, Adams, and Fresco (*9*) that tRNA in the native conformation requires a small number of site-bound divalent cations.

In addition to utilizing tRNA sequence similarities and to matching the experimental x-ray data, the model also agrees with much of the chemical evidence available. The chemically unreactive TψC loop of helix *e* is the least exposed loop, fitting into the groove of helix *c*. Although the small-angle x-ray studies do not warrant placing many restrictions on the unpaired loop regions, it is possible to achieve considerable base-stacking in these regions. The 12 base-pair helix forms a rigid stem on which the remainder of the molecule is folded, and the distance between the anticodon and the CCA-hydroxyl end is constant except for movement of the last four nucleotides of the CCA-hydroxyl end. The anticodon arm, helix *c*, is exposed and free to interact with mRNA in agreement with the evidence of Rudland and Dube (*10*). A molecule of this size and shape will fit the unit-cell packing requirements found in crystallographic studies and is consistent with the projected electron density for crystals of *E. coli* $tRNA^{Leu}$ and yeast $tRNA^{fMet}$ (*11*).

Our model has two important features. (i) Based on the absence, in all sequenced tRNA's, of any unpaired bases between the helical regions *a* and *e*, we have made one continuous helix of 12 base pairs. (ii) Based on small-angle x-ray scattering studies, we have placed the anticodon helix *c* approximately coaxial with the main helix, and the axis of helix *b* at a separation of about 5 Å from it, giving a molecule of dimensions 25 by 35 by 85 Å.

PETER G. CONNORS
MINDAUGAS LABANAUSKAS
Laboratory of Biophysics,
University of Wisconsin,
Madison 53706

W. W. BEEMAN
Department of Physics and
Laboratory of Biophysics,
University of Wisconsin

References and Notes

1. Abbreviations are: tRNA, transfer ribonucleic acid; mRNA, messenger RNA; Ala, alanine; fMet, formylmethionine; Tyr, tyrosine; Phe, phenylalanine; A, adenine; C, cytosine; G, guanine; U, uracil; ψ, pseudouracil; T, ribothymidine; poly C, poly cytidylic acid; poly G, poly guanylic acid; and tris, tris(hydroxymethyl)aminomethane.
2. H. N. Ritland, P. Kaesberg, W. W. Beeman, *J. Appl. Phys.* **21**, 838 (1950).
3. J. A. Lake and W. W. Beeman, *J. Mol. Biol.* **31**, 115 (1968).
4. W. R. Krigbaum and R. W. Godwin, *Macromolecules* **1**, 375 (1968).
5. S. Arnott, M. H. F. Wilkins, W. Fuller, R. Langridge, *J. Mol. Biol.* **27**, 535 (1967).
6. R. Langridge, D. A. Marvin, W. E. Seeds, H. R. Wilson, C. W. Hooper, M. H. F. Wilkins, L. D. Hamilton, *ibid.* **2**, 38 (1960).
7. F. Cramer, H. Doepner, F. v. d. Haar, E. Schlimme, H. Seidel, *Proc. Nat. Acad. Sci. U.S.* **61**, 1385 (1968).
8. W. Fuller and A. Hodgson, *Nature* **215**, 817 (1967).
9. T. Lindahl, A. Adams, J. R. Fresco, *Proc. Nat. Acad. Sci. U.S.* **55**, 941 (1966).
10. P. S. Rudland and S. K. Dube, *J. Mol. Biol.* **43**, 273 (1969).
11. M. Labanauskas, P. G. Connors, J. D. Young, R. M. Bock, J. W. Anderegg, W. W. Beeman, *Science*, this issue.
12. Supported by NIH research and training grants. We thank Oak Ridge National Laboratories for purified *E. coli* $tRNA^{Phe}$. We thank U. L. RajBhandary for samples of yeast $tRNA^{fMet}$, and J. W. Anderegg for advice and assistance.

2 September 1969

Structural Studies on Transfer RNA: Preliminary Crystallographic Analysis

Abstract. *Single-crystal diffraction patterns from* Escherichia coli *leucine tRNA and yeast formylmethionine tRNA show a tetragonal lattice for the former, with* a = *46 Å and* c = *137 Å, and a hexagonal lattice for the latter, with* a = *115 Å and* c = *137 Å. Initial analysis suggests a molecule with a long, double helix parallel to the* c*-axis for both crystals.*

We present a preliminary analysis of x-ray data collected from crystals of $tRNA^{fMet}$ from yeast and $tRNA^{Leu}$ from *Escherichia coli*. Techniques for crystal growth are discussed in an accompanying report (*1*). Precession photographs from both crystals are shown in Fig. 1. The space group of the $tRNA^{fMet}$ crystals is $P6_222$ (or $P6_422$) with unit cell dimensions $a = 115$ Å and $c = 137$ Å. There are 12 molecules in the unit cell and one molecule per asymmetric unit. The space group of the $tRNA^{Leu}$ crystals is $P4_1$ (or $P4_3$) with cell dimensions $a = 46$ Å and $c = 137$ Å. There are four molecules per unit cell and one molecule per asymmetric unit. The resolution of the present data is 10 or 12 Å. The analysis employs model building and Patterson synthesis of the intensities. We discuss here the electron density projected into the basal plane. Only the $F(hk0)$ are involved.

Based on both chemical and physical evidence several models for tRNA have been proposed (*2–4*). Most models, and in particular the one we use (*3*), suggest a prolate asymmetric molecule with the double-helical regions parallel to the long axis. Such a molecule, properly placed in the unit cell with the helix axes parallel to the *c*-axis, gives excellent agreement with the observed Patterson. The electron density projected into the basal plane is centrosymmetric and the $F(hk0)$ phases must be zero or pi. These phases were calculated from a partial model and with the observed intensities give an electron density map that was used as a guide for the arrangement of the rest of the molecule. The results suggest a molecule containing a long double-helical region around which the rest of the molecule is rather compactly folded. Most of our analysis is on $tRNA^{Leu}$, but the same model gives good agreement with the data on $tRNA^{fMet}$.

Figure 2a shows the Patterson synthesis of the experimental intensities of the centrosymmetric $hk0$ plane of the